Ab initio Quantum and *ab initio* Molecular Dynamics of the Dissociative Adsorption of Hydrogen on Pd(100)

Axel Gross and Matthias Scheffler
Fritz-Haber-Institut der Max-Planck-Gesellschaft, Faradayweg 4-6, D-14195 Berlin-Dahlem, Germany
(May 2, 1997)

The dissociative adsorption of hydrogen on Pd(100) has been studied by *ab initio* quantum dynamics and *ab initio* molecular dynamics calculations. Treating all hydrogen degrees of freedom as dynamical coordinates implies a high dimensionality and requires statistical averages over thousands of trajectories. An efficient and accurate treatment of such extensive statistics is achieved in two steps: In a first step we evaluate the *ab initio* potential energy surface (PES) and determine an analytical representation. Then, in an independent second step dynamical calculations are performed on the analytical representation of the PES. Thus the dissociation dynamics is investigated without any crucial assumption except for the Born-Oppenheimer approximation which is anyhow employed when density-functional theory calculations are performed. The *ab initio* molecular dynamics is compared to detailed quantum dynamical calculations on exactly the same *ab initio* PES. The occurence of quantum oscillations in the sticking probability as a function of kinetic energy is addressed. They turn out to be very sensitive to the symmetry of the initial conditions. At low kinetic energies sticking is dominated by the steering effect which is illustrated using classical trajectories. The steering effects depends on the kinetic energy, but not on the mass of the molecules. Zero-point effects lead to strong differences between quantum and classical calculations of the sticking probability. The dependence of the sticking probability on the angle of incidence is analysed; it is found to be in good agreement with experimental data. The results show that the determination of the potential energy surface combined with high-dimensional dynamical calculations, in which all relevant degrees of freedon are taken into account, leads to a detailed understanding of the dissociation dynamics of hydrogen at a transition metal surface.

68.35.Ja, 82.20.Kh, 82.65.Pa

I. INTRODUCTION

The dissociative adsorption of molecules on surfaces is one of the fundamental reaction steps occuring in catalysis, corrosion, and in the hydrogen gas storage in metals. Adsorption corresponds to a process in which statistically distributed molecules hit the surface from the gas phase. For a diatomic molecule this requires the calculation of thousands of trajectories; the adsorption probability is then obtained by averaging over these trajectories. In "traditional" *ab initio* molecular dynamics the electronic structure, total energy and the forces acting on the nuclei are determined for each configuration *during the journey* of the particles which requires of the order of 100 – 1000 self-consistent calculations for each trajectory. Since the determination of total energies and forces is still a heavy computational task, the number of trajectories obtainable in such a "during the journey" *ab initio* molecular dynamics simulation is limited to numbers well below 100.[1,2] These numbers are too low to achieve a reasonable statistics. Typically one needs to consider of the order of 10^3 to 10^5 trajectories, depending on the kind of experiment to be simulated.[3] Therefore we propose a "divide and conquer" approach for *ab initio* molecular dynamics: At first the road map should be created and only then the journey started. Thus, in a first (elaborate) study we analyse the *ab initio* potential energy surface (PES). This PES is parametrized in a suitable form and only then the molecular dynamics calculations are performed on the analytical representation of the *ab initio* potential. In this way it is easy to study up to 10^6 trajectories.

If hydrogen is involved in the dissociation process, quantum effects may play a role in the dynamics. We have recently improved a quantum dynamical algorithm that makes it possible to treat *all* six degrees of freedom of the hydrogen molecule in the dissociation process quantum dynamically.[4] Quantum effects can thus be determined by comparing the results of the quantum dynamical calculations with classical trajectory calculation on exactly the same PES. It turns out that for hydrogen moving on a strongly corrugated and anisotropic PES zero-point effects can be substantial.[3] One advantage of the quantum dynamics, that to our knowledge has not been emphasized in the literature yet, is that the averaging over the initial conditions is done automatically. For example, a plane wave in a $j = 0$ rotational state describing the incident molecular beam hits the surface everywhere in the surface unit cell and contains all molecular orientations with equal probability.

Dissociative adsorption systems can be roughly divided into two classes[5,6,7,8,9]: Systems, where the sticking probability is monotonously increasing as a function of the incident kinetic energy of the impinging molecules, and systems, where the sticking probability shows an initial decrease with increasing kinetic energy. The in most detail studied system H_2/Cu[10,11,12,13,14,15,16,17,18,19,20,21,22,23,24] belongs to the first class. These systems are characterized by a minimum barrier hindering dissociative adsorption, so that

increasing the kinetic energy helps to overcome the barrier.

The second class consists of adsorption systems like H_2[25,26,27,28,29,30,31], O_2[32,33,34,35], and N_2[36] on various transition metal surfaces. In particular the well-studied system H_2/Pd(100),[5,7,25,37,38,39] which is the subject of our study, belongs to this class. An initially decreasing sticking probability had usually been explained by a *precursor mechanism*.[5] In this concept the molecules are temporarily trapped in a molecular physisorption state, the so-called *precursor state*, before they dissociatively adsorb. The energy dependence of the sticking probability is related to the trapping probability into the precursor state. It is this trapping probability which decreases with increasing energy.[5]

However, it has for example been shown for the system H_2/W(100)–c(2×2)Cu[30] that for a hydrogen molecule impinging on a metal substrate the energy transfer to substrate phonons is much too small to account for the high sticking probabilities at low kinetic energies due to the large mass mismatch. Therefore also direct non-activated adsorption together with a steering effect has been suggested in order to explain the initial decrease of the sticking probability by King almost twenty years ago[40]. Still, in low-dimensional dynamical treatments of the H_2/Pd(100) system no steering effect was observed.[37,38,39] Only very recently it has been shown by high-dimensional quantum dynamical calculations based on *ab initio* potential energy surfaces (PES) for the systems H_2/Pd(100)[4,8,41] and H_2/W(100)[42,43] that indeed an initial decrease of the sticking probability with increasing kinetic energy is not necessarily due to a precursor mechanism. For both systems the PES has non-activated paths towards dissociative adsorption and no molecular adsorption well. However, the majority of pathways towards dissociative adsorption has in fact energy barriers with a rather broad distribution of heights and positions, i.e. the PES is strongly anisotropic and corrugated. Similiar features of the potential have recently been found also for the interaction of H_2 with Rh(100).[44] A slow molecule moving on such a PES with an unfavorable initial configuration for dissociative adsorption can be steered efficiently towards non-activated paths to adsorption by the forces acting upon the molecule. This mechanism becomes less efficient at higher kinetic energies because then the molecule is too fast to be diverted significantly. More particles are therefore scattered back into the gas-phase from the repulsive part of the potential. This leads to the initial decrease of the sticking probability. At even higher kinetic energies the molecule will eventually have enough energy to directly traverse the barriers causing the sticking probability to rise again.

In our calculations for the interaction of H_2/Pd(100) *all* six degrees of freedom of the hydrogen molecule are treated dynamically[4]. This makes it possible to investigate the influence of *all* hydrogen degrees of freedom on the dissociative adsorption, scattering and associative desorption on an equal footing. So far we have studied the dependence of adsorption and desorption on kinetic energy, molecular rotation and orientation[4,45], molecular vibration[46], ro-vibrational coupling[47] and the rotationally elastic and inelastic diffraction of H_2/Pd(100)[48].

In this article we will first describe the quantum and classical methods we have used to determine the adsorption dynamics of hydrogen on Pd(100). Then we address the origin of oscillations in the sticking probability as a function of the kinetic energy. Next the steering effect is illustrated and the differences between classical and quantum dynamics are discussed as are isotope effects in the dissociative adsorption dynamics. Finally we will focus on the dependence of the sticking probability on the angle of incidence.

II. COMPUTATIONAL DETAILS

In our approach the dynamical simulations including all relevant degrees of freeedom are performed on an analytical representation of the *ab initio* PES. Thus in principle we apply only one approximation, namely the Born-Oppenheimer approximation, i.e., we assume that the electrons follow the motion of the nuclei adiabatically. Obviously in practice there is a second important approximation, namely the treatment of the exchange and correlations effects in the density functional theory calculations.

As far as the number of relevant degrees of freedom is concerned, in the case of hydrogen dissociation on densely packed metal surfaces usually no significant surface rearrangement upon adsorption occurs, and there is only a small energy transfer from the light hydrogen molecule to the heavy substrate atoms. Even if there is any surface relaxation upon hydrogen adsorption, it occurs typically on a much larger time scale than the adsorption event. The crucial process in the dissociative adsorption for these particular systems is therefore the conversion of translational and internal energy of the hydrogen molecule into translational and vibrational energy of the adsorbed hydrogen atoms. Thus the dissociation dynamics can be described by a six-dimensional PES which takes only the molecular degrees of freedom into account. In the following we present our formalism in such a six-dimensional formulation. In principle, however, it can be extended to include also the substrate degrees of freedom if they are relevant.

A. Parametrization of the *ab initio* potential

In order to obtain a reasonable analytical representation of the PES, first a sufficient number of *ab initio* total energies has to be computed. High-symmetry points of the multi-dimensional configuration space are reflected

by extrema in the PES. Typically in between the high-symmetry points the PES is smooth and has no additional maxima and minima. Of course, this assumption has to checked carefully. In the case of a rigid surface, the PES of a diatomic molecule interacting with this surface is a function of the six molecular degrees of freedom. They can be represented, e.g., by the center-of-mass coordinates X, Y, Z, the interatomic distance r, and the polar and azimuthal angle of the molecular axis θ and ϕ. Figure 1 shows a two-dimensional cut through the six-dimensional coordinate space of H_2/Pd (100), a so-called elbow plot. The two considered coordinates are the H_2 center-of-mass distance from the surface Z and the H-H interatomic distance r.

In order to solve the time-independent Schrödinger equation describing dissociative adsorption it is advantageous to transform the coordinates in the Zr-plane into reaction path coordinates s and ρ[49,50,51]. Here s describes the position along the "reaction path" – the dashed line in Fig. 1 – and ρ is the coordinate perpendicular to s (see section II B). We have then parametrized the function $V(X, Y, s, \rho, \theta, \phi)$, which describes the potential energy surface on which the hydrogen molecule moves, in the following form:[4]

$$V\ (X, Y, s, \rho, \theta, \phi)\ =\ V^{\rm corr}\ +\ V^{\rm rot}\ +\ V^{\rm vib} \qquad (1)$$

with

$$V^{\rm corr}\ =\ \sum_{m,n=0}^{2} V^{(1)}_{m,n}(s)\ \cos mGX\ \cos nGY, \qquad (2)$$

$$V^{\rm rot} = \sum_{m=0}^{1}\ V^{(2)}_{m}(s)\ \frac{1}{2}\cos^2\theta\ (\cos mGX + \cos mGY)$$

$$+\sum_{n=1}^{2}\ V^{(3)}_{n}(s)\ \frac{1}{2}\sin^2\theta\ \cos 2\phi\ (\cos nGX - \cos nGY) \quad (3)$$

and

$$V^{\rm vib}\ =\ \frac{\mu}{2}\ \omega^2(s)\ [\rho\ -\ \Delta\rho(X, Y, s)]^2\ . \qquad (4)$$

$G = 2\pi/a$ is the length of the basis vectors of the square surface reciprocal lattice, a is the nearest neighbor distant between Pd atoms and $\omega(s)$ is the vibrational frequency. We note that Wiesenekker *et al.*[52] have recently employed an equivalent analytic representation to describe the 6D-PES of H_2/Cu(100), the only difference being that they use cartesian coordinates in the Zr-plane instead of reaction path coordinates.

It turns out that the calculation of total energies for 250 different configurations is sufficient to determine the parameters necessary to describe the functions appearing in the potential parametrization. The *ab initio* energies are obtained[41] using density functional theory together with the generalized gradient approximation (GGA)[53] for the exchange and correlation functinal and the full-potential linear augmented plane wave method (FP-LAPW) (see Ref. 54 and references therein). The ten functions $V^{(i)}_{m,n}(s)$ and $\omega(s)$ are determined such that the difference to the *ab initio* calculations on the average is smaller than 25 meV.

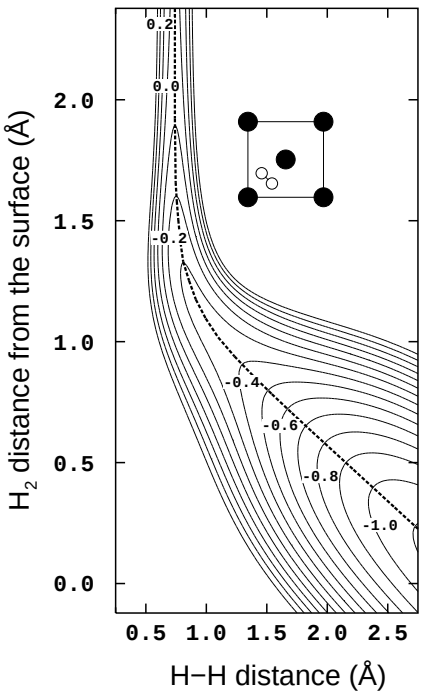

FIG. 1. Contour plot of the PES along a two-dimensional cut through the six-dimensional coordinate space of H_2/Pd (100). The inset shows the orientation of the molecular axis and the lateral H_2 center-of-mass coordinates, i.e. the coordinates X, Y, θ, and ϕ. The coordinates in the figure are the H_2 center-of-mass distance from the surface Z and the H-H interatomic distance r. The dashed line is the optimum reaction path. Energies are in eV per H_2 molecule. The contour spacing is 0.1 eV.

The introduction of the displacement $\Delta\rho$ in the potential term $V^{\rm vib}$ (Eq. 4) takes into account that the location of the minimum energy path in the Zr-plane depends on the cut through the six-dimensional configuration space of H_2/Pd(100). $\Delta\rho$ does not influence the barrier distribution, however, it changes the curvature of the minimum energy paths in the Zr-planes. For the calculated elbow plots $\Delta\rho$ reaches values of up to 0.6 Å, but only for large separations of the hydrogen atoms, i.e., when the molecule is already dissociated. Large values of $\Delta\rho$ require a large number of vibrational eigenfunctions in the expansion of the hydrogen wave function in the coupled channel scheme (see below), which makes the calculations very time-consuming. Since the large values of $\Delta\rho$ occur only for large separations of the hydrogen atoms, they do not influence the calculated sticking probabilities and scattering properties significantly, as we have checked by test calculations. We have therefore parametrized the

displacement properly only for values of $|\Delta\rho| \leq 0.15$ Å.

B. Quantum dynamics

The Hamiltonian of a hydrogen molecule interacting with a rigid surface can be written as

$$H \;=\; -\frac{\hbar^2}{2M}\,\nabla^2_{\mathbf{R}} \;-\; \frac{\hbar^2}{2\mu}\,\nabla^2_{\mathbf{r}} \;+\; V(\mathbf{R},\mathbf{r})\;. \tag{5}$$

$\mathbf{R} = (\mathbf{r}_1 + \mathbf{r}_2)/2 = (X, Y, Z)$ and $\mathbf{r} = (\mathbf{r}_2 - \mathbf{r}_1)$ are the center-of-mass and relative coordinates of the hydrogen molecule, respectively, $M = 2m$ and $\mu = m/2$ are the total and reduced mass of the hydrogen molecule, respectively, where m is the mass of a hydrogen atom. Now we write the relative part in spherical coordinates; with $r = |\mathbf{r}|$ this yields

$$\begin{aligned} H = &-\frac{\hbar^2}{2M}\,\nabla^2_{\mathbf{R}} \;-\; \frac{\hbar^2}{2\mu}\,\left(\frac{\partial^2}{\partial r^2} \;+\; \frac{2}{r}\frac{\partial}{\partial r} \;-\; \frac{\mathbf{L}^2}{r^2}\right) \\ &+ V(\mathbf{R}, r, \theta, \phi)\;, \end{aligned} \tag{6}$$

where $\mathbf{L}$ is the angular momentum operator.

We define r_e as the equilibrium bond length for a certain molecular configuration, i.e., r_e is in general a function of the five coordinates X, Y, Z, θ and ϕ. The vibrational amplitude of diatomic molecules is usually small compared to the equilibrium bond length, which means that

$$|r_e - r| \;\ll\; r\;. \tag{7}$$

This allows us[55] to neglect the term $\frac{2}{r}\frac{\partial}{\partial r}$ in the Hamiltonian and to approximate the angular momentum term by $\frac{\mathbf{L}^2}{r^2} \approx \frac{\mathbf{L}^2}{r_e^2}$. Then we end up with the following Hamiltonian

$$\begin{aligned} \tilde{H} = &-\frac{\hbar^2}{2M}\,\nabla^2_{\mathbf{R}} \;-\; \frac{\hbar^2}{2\mu}\,\left(\frac{\partial^2}{\partial r^2} \;-\; \frac{\mathbf{L}^2}{r_e^2}\right) \\ &+ V(\mathbf{R}, r, \theta, \phi)\;, \end{aligned} \tag{8}$$

As already mentioned in section II A, it is advantageous to transform the coordinates in the Zr-plane into reaction path coordinates s and ρ in order to solve the time-independent Schrödinger equation describing dissociative adsorption. To perform the transformation to the reaction path coordinates, first Z has to be mass-scaled to the coordinate z by

$$z \;=\; Z\,\sqrt{\frac{M}{\mu}}\;. \tag{9}$$

The PES in Fig. 1 is already plotted according to mass-scaled coordinates. With the reaction path coordinates s and ρ the Hamiltonian becomes

$$\begin{aligned} \tilde{H} = &-\frac{\hbar^2}{2\mu}\,\left(\eta^{-1}\frac{\partial}{\partial s}\left(\eta^{-1}\frac{\partial}{\partial s}\right) \;+\eta^{-1}\frac{\partial}{\partial \rho}\left(\eta\frac{\partial}{\partial \rho}\right)\right) \\ &-\frac{\hbar^2}{2\mu}\,\left(\frac{\partial^2}{\partial r^2} \;-\; \frac{\mathbf{L}^2}{r_e^2}\right) \\ &-\frac{\hbar^2}{2M}\,\left(\frac{\partial^2}{\partial X^2} + \frac{\partial^2}{\partial Y^2}\right) + \;V(X, Y, s, \rho, \theta, \phi)\;. \end{aligned} \tag{10}$$

The coupling parameter η is defined by

$$\eta \;=\; 1 \;-\kappa(s)\;\rho\;, \tag{11}$$

where $\kappa(s)$ is the curvature of the lowest energy reaction path (the dashed line in Fig. 1).

The displacement $\Delta\rho$ also enters the denominator of the angular momentum term in the Hamiltonian via the equilibrium bondlength r_e

$$r_e \;=\; r_e^0(s) \;+\; \sin\phi_r(s)\;\Delta\rho(X, Y, s)\;. \tag{12}$$

Here $\sin\phi_r(s)$ is the angle between the reaction path (dashed line in Fig. 1) and the z-axis. Since the relation

$$\sin\phi_r(s)\;\Delta\rho(X, Y, s) \;\ll\; r_e^0(s) \tag{13}$$

holds, we have expanded r_e^{-2} in the angular momentum term in a Taylor series in $\sin\phi_r(s)\;\Delta\rho(X, Y, s)$ up to second order.

The quantum dynamical calculations are performed by solving the time-independent Schrödinger equation for the two hydrogen nuclei moving on the six-dimensional PES in a coupled-channel scheme. As channels the eigenfunctions of the Hamiltonian for molecules in the gas phase are used. We use the concept of the *local reflection matrix* (LORE)[39,56]. For a detailed description of this stable coupled channel method we refer to Refs. 39 and 56. In the LORE scheme the reflection matrix R is determined; in order to obtain sticking probabilities S_i for some initial state i, where i stands for a multi-index, we use unitarity:

$$S_i \;=\; 1 \;-\; \sum_j |R_{ji}|^2\;. \tag{14}$$

R_{ji} is the differential reflection amplitude; the sum over j extends over all possible reflection states.

The basis set used in the coupled-channel algorithm for the H_2 results presented here included rotational eigenfunctions with rotational quantum numbers up to $j_{\max} = 8$, vibrational eigenfunctions with vibrational quantum numbers up to $v_{\max} = 2$, and parallel momentum states with maximum parallel momentum $p_{\max} = 7\hbar G$ with $G = 2\pi/a$. The convergence of the results with respect to the basis set has been carefully checked by calculations with maximum quantum numbers $j_{\max} = 10$, $v_{\max} = 3$, and $p_{\max} = 10\hbar G$, respectively.

Due to the higher mass of D_2 the energy spacing between the quantum levels is smaller for D_2 than for H_2. Therefore much more eigenfunctions in the expansion of the wavefunction have to be taken into account

in the coupled-channel calculations for D_2 than for H_2. This makes a six-dimensional quantum treatment of D_2 very time-consuming. In order to investigate isotope effects we have therefore performed five-dimensional vibrationally adiabatic quantum calculations for D_2, where the molecules are not allowed to make vibrational transitions. We have already shown that vibrationally adiabatic calculations are very close to the full six-dimensional results for the dissociation of H_2 on Pd(100)[46]. This should also be valid for D_2 since the ratio of the vibrational timescale to the other time-scales of rotation and translation is the same for H_2 and D_2. The five-dimensional quantum calculations for D_2 have been performed with rotational quantum states up to $j_{\max} = 12$ and parallel momentum states with $p_{\max} = 11\hbar G$.

In coupled-channel calculations always the whole S-matrix has to be computed. This leads to a N^3-scaling of the algorithm due to the matrix operations, where N is the number of channels included in the calculation. In order to perform these demanding quantum dynamical calculations it is therefore necessary to utilize the symmetries of the scattering problem (see also Ref. 57). First of all selections rules are important. Because of the inversion symmetry of the H_2 molecule only rotational transition with $\Delta j = even$ are allowed, where j is the rotational quantum number. In addition, the analytic representation of PES only contains rotational potential terms that cause $\Delta m = even$ transitions (see the second sum of V^{rot} in Eq. 3), where m is the azimuthal quantum number of the H_2 molecule.

Furthermore, we exploit the symmetry group of the Hamiltonian which corresponds to the C_{4v} symmetry of the fcc (100)-surface. In general the scattering solutions do not belong to irreducible representations of the symmetry group. However, if the scattering solutions of interest can be decomposed into irreducible representations, the number of relevant channels per coupled-channel calculation can be significantly reduced. This is due to the fact that only channels belonging to the same irreducible representation of the symmetry group couple to each other, since the Hamiltonian commutes with the symmetry operator.

If, for example, the incident parallel momentum corresponds to a reciprocal lattice vector (this includes the zero-vector for normal incidence) and the initial rotational quantum number j and the azimuthal quantum number m are even, the scattering solutions can be broken up into eight different irreducible representations of the symmetry group, four of which can be further decomposed. In each decomposition the number of channels is roughly halved, and in each irreducible representation the S-matrix is calculated separately. This leads to a reduction of the computational cost to approximately $4 \cdot (1/8)^3 + 8 \cdot (1/16)^3 = 5/512 \approx 1.0\%$. If only the sticking probability for normal incidence is required, it is sufficient to calculate only two S-matrices, i.e., the exploitation of the symmetries causes a reduction in the CPU time to $\sim 2 \cdot (1/16)^3 = 1/2048 \approx 0.05\%$. Without the use of the symmetry the calculations presented here would not be feasible. Using the selection rules and the decomposition into irreducible representations up to 25,000 channels per total energy are taken into account in the quantum dynamical calculations; the actual number of channels in the single calculations is usually $\lesssim 600$. For a more detailed description of the construction of symmetry adapted channels, see Ref. 57.

C. Classical dynamics

The classical trajectory calculations are performed on *exactly the same* PES as the quantum dynamical calculations. To derive the classical equations of motion from the reaction path Hamiltonian Eq. 10 we have used[58]

$$\begin{aligned} -i\hbar\, \partial_s &\equiv p_s \ , \\ -i\hbar\, \partial_\rho &\equiv p_\rho \ . \end{aligned} \tag{15}$$

The equations of motions are numerically integrated with the Bulirsch-Stoer method with a variable time-step[59]. We required that the energy conservation per molecular dynamics run was fulfilled to 0.1 meV. The sticking probability is determined by averaging over a sufficient number of trajectories. The exact number of trajectories to be considered depends on the specific initial conditions and ranges between 1,815 and 18,330.

As far as the CPU time requirement is concerned, it is a wide-spread believe that classical methods are much less time-consuming than quantum ones. This is certainly true if one compares the computational cost of one trajectory to a quantum calculation. However, since in quantum mechanics the averaging over initial conditions is done automatically while in classical mechanics one has to average over many trajectories corresponding to different initial conditions, for the results presented here the quantum method is even more time-efficient than the classical calculations, in particular if one considers the fact, that in a coupled-channel method the sticking and scattering probabilites of all open channels are determined simultaneously.

III. RESULTS AND DISCUSSION

A. Quantum oscillations

Figure 2 presents six-dimensional quantum dynamical calculations of the sticking probability as a function of the kinetic energy of a H_2 beam under normal incidence on a Pd(100) surface and five-dimensional calculations for D_2. In addition, the results of the H_2 molecular beam experiment by Rendulic, Anger and Winkler[25] are shown.

First of all a very strong oscillatory structure is apparent in the sticking probability as a function of the incident energy. Such structures reflect the quantum nature of the scattering. They are known for a long time in

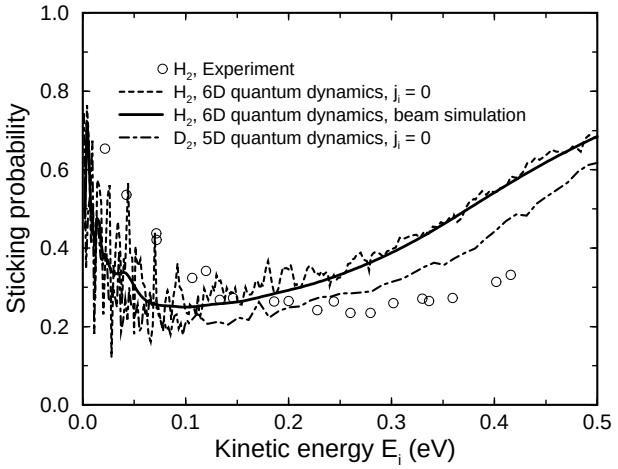

FIG. 2. Sticking probability versus kinetic energy for a hydrogen beam under normal incidence on a Pd(100) surface. Experiment (H_2): circles (from ref. 25); theory: six-dimensional results for H_2 molecules initially in the rotational and vibrational ground state (dashed line) and with an initial rotational and energy distribution adequate for molecular beam experiments (solid line), and vibrationally adiabatic five-dimensional results for D_2 molecules initially in the rotational ground state (dash-dotted line).

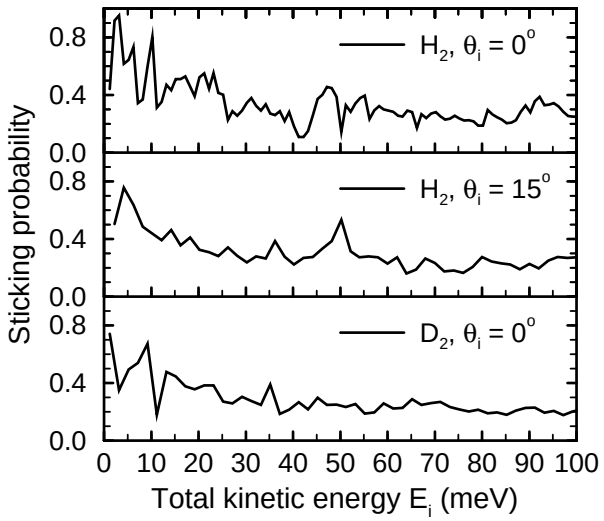

FIG. 3. 5D quantum calculations of the sticking probability versus kinetic energy for a hydrogen beam impinging on a Pd(100) surface. Upper panel: H_2 under normal incindence $\theta_i = 0°$; Middle panel: H_2 with an incident angle of $\theta_i = 15°$; Lower panel: D_2 under normal incidence $\theta_i = 0°$.

He and H_2 scattering[60] and also in LEED[61]. In the case of the sticking probability of H_2/Pd(100), these oscillations have been the issue of a current debate[48,62,63,64]. We have recently shown[48] that the peaks in the sticking probability can be related to the opening up of new scattering channels with increasing kinetic energy, especially at low kinetic energies. In particular the emergence of the [10], [11], and [20] diffraction channels for normal incidence and the opening up of rotational excitation lead to strong peaks in the sticking probablity. Here $[n, m]$ corresponds to the diffraction indices of the (100)-surface.

Rettner and Auerbach[62,64] have tried to find the theoretically predicted oscillations[4] by an effusive beam experiment, but they could not detect any. As pointed out,[48,63] the height of the peaks is very sensitive to the symmetry of the scattering conditions. Surface imperfections like adatoms and steps and also the thermal motion of the substrate will reduce the coherence of the scattering process and thus smooth out the oscillatory structure. But more importantly, also the angle of incidence has a decisive influence on the symmetry.

The experiment by Rettner and Auerbach was done for an angle of incidence of 15°, while the calculations were done for normal incidence. In order to investigate the dependence of the oscillatory structure on the angle of incidence we performed five-dimensional vibrationally adiabatic calculations for an angle of incidence of the molecular beam of 15° and compared them with normal-incidence results (see Fig. 3). The energy resolution for the non-normal incidence results was chosen to be below the width of the prominent peaks for normal incidence so that these peaks should be detected. In order to rule out basis set effects, also the results for normal incidence in Fig. 3 were obtained by five-dimensional calculations. Caused by the reduced dimensionality, the height of the peaks for normal incidence is changed compared to the full six-dimensional calculations. This indicates the importance of the full dimensionality for the calculations. The peak positions, however, are the same. Also the averaged sticking probability is not changed significantly[46].

Now at normal incidence every diffraction channel is at least fourfold degenerate (except for the backscattered beam) due to the C_{4v} symmetry of the (100) surface. This makes the effect of the opening up of a new scattering channel much more dramatic than in the case of a general angle of incidence, where this degeneracy is lost. This is demonstrated in Fig. 3, which shows that in the energy regime below 40 meV, which was probed by Rettner and Auerbach,[62,64] the sticking probability for $\theta_i = 15°$ is much smoother than for normal incidence. Thus, as expected, calculations for normal incidence are not directly comparable with experiments for non-normal incidence, at least as far as quantum effects are concerned.

The large peak at approximately $E_i \approx 50$ meV is still visible for both angles of incidence. This peak is due to the opening up of rotationally inelastic diffraction, i.e., the kinetic energy becomes large enough to enable $j = 0 \rightarrow 2$ rotational transitions in scattering. For $\theta_i = 15°$ this peak is slightly shifted to higher *total* kinetic energies. This is simply due to the fact that the

rotationally inelastic *specular* peak opens up at higher total kinetic energy due to the parallel momentum conservation.

In recent quantum dynamical calculations of the dissociative adsorption of the reactive system $H_2/W(100)$[42] also oscillations in the sticking probability were found, but they were much smaller than for $H_2/Pd(100)$. This may be caused by the lower dimensionality of these calculations. Since only one surface coordinate was considered, the number of degenerate scattering channels opening up was less than in six-dimensional calculations, leading to smaller effects. For example, in previous quantum dynamical calculations of the dissociative adsorption of H_2 on a model potential with activated as well as non-activated paths to adsorption, where also only one surface coordinate was considered, quantum oscillations have also been found,[8] there amplitude, however, is much smaller than in the 6D-calculations.

For the heavier isotope D_2 the energetic spacing between quantum levels is much less due to the higher mass compared to H_2. The higher "density" of channels should also make the effects of the opening up of new scattering channels less dramatic. In the lower panel of Fig. 3 we have plotted five-dimensionals results for the D_2 sticking probability under normal incidence with the same energy resolution as for the H_2 non-normal incidence results. Except for low kinetics energies the sticking curve is indeed much smoother than for H_2 at normal incidence.

There is a further source for the smoothening of the sticking probability as a function of the incident kinetic energy in supersonic molecular beam experiments: The experimental beam does not correspond to a monoenergetic beam in one specific quantum state. Instead, there is a certain velocity spread of the impinging molecules which is typically of the order of $\Delta v/v_i = 0.1$, where v_i is the mean initial velocity[25]; in addition, the internal states of the molecules are populated according to some Boltzmann-like distribution. For the solid line in Fig. 2 we have assumed an initial rotational and energy distribution adequate for molecular beam experiments. As a consequence, the oscillatory structure is almost entirely washed out. Accordingly, also the experimental data of Ref. 25 do not show any significant oscillations.

B. Steering effect

We will now discuss the general trends in the averaged sticking probability as a function of the kinetic energy. The qualitative features of the experimental sticking probability[25] are well reproduced by the averaged quantum dynamical results, as Fig. 2 shows, although there are quantitative differences which we will address below. At low energies there is a substantial decrease in the sticking probability with increasing kinetic energy, which is then followed by an increase at higher kinetic energies. As already pointed out above, such a general behavior had usually been attributed to a precursor mechanism, in which the impinging molecules prior to dissociation are first trapped in a physisorption well due to energy transfer to substrate phonons[5]. This mechanism, however, cannot explain the quantum dynamical results since first, there is no physisorption well in the calculated PES, and second, there is no energy transfer to the surface possible due to the use of a fixed substrate. Thus the decrease in the sticking probability has to be caused by a purely dynamical effect, namely the steering effect:[8,40,4,41,42,43] Although the majority of pathways to dissociative adsorption has non-vanishing barriers with a rather broad distribution of heights and positions, slow molecules can be very efficiently steered to non-activated pathways towards dissociative adsorption by the attractive forces of the potential. This mechanism becomes less effective at higher kinetic energies where the molecules are too fast to be focused into favourable configurations towards dissociative adsorption. If the kinetic energy is further increased, the molecules will eventually have enough energy to directly traverse the barrier region leading to the final rise in the sticking probability.

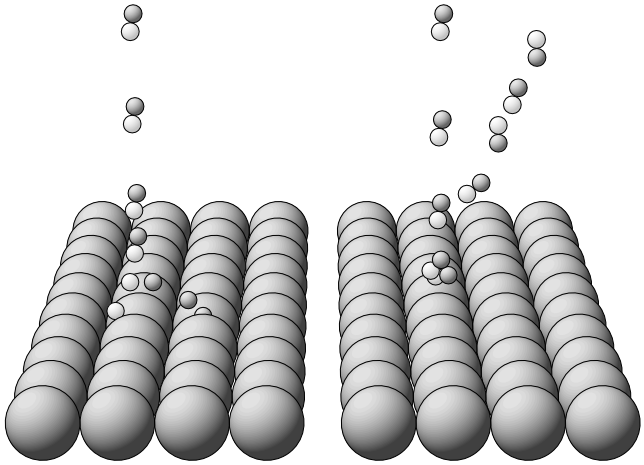

FIG. 4. Snapshots of classical trajectories of hydrogen molecules impinging on a Pd(100) surface. The initial conditions are chosen in such a way that the trajectories are restricted to the xz-plane. Left trajectory: initial kinetic energy $E_i = 0.01$ eV. Right trajectory: same initial conditions as in the left trajectory except that the molecule has a higher kinetic energy of 0.12 eV.

In order to illustrate the steering effects, we use the results of two typical classical trajectory runs. This is done in Fig. 4, where snapshots of these two trajectories are shown. The initial conditions are chosen in such a way that the trajectories are restricted to the xz-plane. The left trajectory illustrates the steering effect. The incident kinetic energy is $E_i = 0.01$ eV. Initially the molecular axis is almost perpendicular to the surface. In such a configuration the molecule cannot dissociate at the sur-

face. But the molecule is so slow that the forces acting upon it can reorient the molecule. It is turned parallel to the surface and then follows a non-activated path towards dissociative adsorption.

In the case of the right trajectory, the initial conditions are the same as in the left one, except that the molecule has a higher kinetic energy of 0.12 eV. Due to the anisotropy of the PES the molecule also starts to rotate to a configuration parallel to the surface. However, now the molecule is so fast that it hits the repulsive wall of the potential before it is in a favorable configuration to dissociative adsorption. It is then scattered back into the gas-phase rotationally excited.

Fig. 2 shows that there are still quantitative differences betweeen theory and experiment. Considering the fact that there are no adjustable parameters in our calculations, the agreement is quite satisfactory, though. The discrepancies might be due to uncertainties in the determination of the *ab initio* PES which are of the order of ± 0.1 eV[41]. We also like to point out that the experimental values of the sticking probability are subject of a current debate[25,64].

Furthermore, in our calculations substrate phonons or electronic excitations are not taken into account. We have noted above that due to the large mass mismatch between impinging hydrogen molecule and the Pd substrate atoms the substrate motion can be neglected as far as understanding the basic dissociation mechanism is concerned. Taking the substrate motion into account would allow for recoil of the surface atoms upon impact of the impinging molecules. Although the energy transfer to the solid is rather small, recoil of the surface atoms leads to a sticking curve which is stretched to higher energies[65,66]. In other words, it renormalizes the energy axis, because due to the energy transfer to the surface the effective kinetic energy becomes smaller. Such a renormalization would improve the agreement between experiment and theory, as an inspection of Fig. 2 reveals.

C. Comparison quantum-classical dynamics and isotope effects

In Fig. 5 we compare the averaged quantum mechanical sticking probability for H_2 with the results of classical and quasiclassical trajectory calculations for H_2 and D_2. The inset shows an enlargement of the results at low energies. Quasiclassical in this context corresponds to trajectories with the initial vibrational energy of the hydrogen molecule equal to the vibrational zero-point energy of hydrogen, which is 0.258 eV for H_2 and 0.185 eV for D_2, while for the purely classical trajectories the molecules are initially non-vibrating. First of all, the classical results do not show any oscillatory structure revealing that the oscillations are entirely due to quantum mechanics. Note that the quasiclassical calculations for H_2 show almost no initial decrease in the sticking probability. For

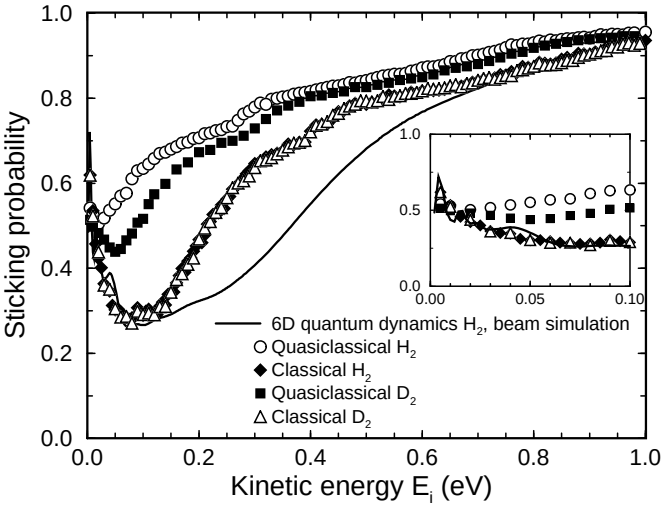

FIG. 5. Probability for dissociative adsorption versus kinetic translational energy for a hydrogen beam under normal incidence on a clean Pd(100) surface for non-rotating molecules. The solid line shows six-dimensional quantum dynamical results for H_2 assuming an energy spread typical for beam experiments. The quasiclassical results corresponds to molecules initially vibrating with an energy equal to the vibrational zero-point energy while the classical results are obtained with initially non-vibrating molecules. Open diamonds: quasiclassical H_2; filled diamonds: classical H_2; filled squares: quasiclassical D_2; open triangles: classical D_2. The inset shows an enlargement of the results at low energies.

D_2 there is a small decrease, while the purely classical results effectively fall upon the averaged H_2 quantum results at low and high kinetic energies.

We have recently shown that the strong difference between quasiclassical results on the one side and classical and averaged quantum results on the other side is caused by zero-point effects of the hydrogen molecule in the multi-dimensional configuration space[3]. When the molecule approaches the surface, the molecular bond is weakened and consequently the molecular vibration is softened, i.e., the vibrational frequency decreases. Since the change of the frequency is slow compared to the vibrational period, the vibrational energy follows the change of the frequency almost adiabatically[3,46] which leads to an effective vibrational-translational energy transfer. At the same time, due to the anisotropy and corrugation of the PES the molecule about to dissociate becomes localized in the remaining four degrees of freedom of the molecule which are the polar and azimuthal rotation and the two translations parallel to the surface. This localization leads to the building up of additional zero-point energies due to the Heisenberg uncertainty principle. In fact, the sum of all zero-point energies remains approximately constant along a minimum energy path towards dissociative adsorption[67,68], and for H_2/Pd(100) the sum becomes even larger than the gas-phase vibrational zero-point energy of H_2, which is the

only zero-point energy of a free molecule.

Now a classical particle can follow precisely a minimum energy path through a corrugated PES; in a pictorial sense one might say it can propagate along the bottom of the valley in the PES. A quantum particle cannot do that. It has to be delocalized and needs to have at least the zero-point energies perpendicular to the propagation direction to traverse a corrugated PES without tunneling. This leads to an effective upwards shift of the potential for the quantum particle along the minimum energy path. Or *vice versa*, the classical particle experiences a lower minimum potential. As a consequence, the sticking probability for the quasiclassical particle is much larger than for the quantum particle.

As mentioned above, the sum of all zero-point energies along the minimum energy path towards dissociation adsorption increases in the systen H_2/Pd(100), but in a first approximation we assume it to be roughly constant. In such a situation the combined effect of all zero-point energies is to cause a constant shift of the potential. Therefore the results of quantum calculations and classical calculations without any initial zero-point energy should be similiar since a constant shift of the potential does not affect the dynamical properties. This is indeed the case at low and at high energies, as the comparison between purely classical and quantum results in Fig. 5 demonstrates. In addition, these results confirm that steering is a general dynamical effect and is not particularly related to quantum or classical dynamics.

The problem of a proper treatment of zero-point energies in quasiclassical trajectory calculations is well-known, especially in the gas-phase community[69,70]. One possible way to deal with this problem is the reduced dimensionality treatment in the vibrationally adiabatic approximation (for a overview see Ref. 71). In this approach a small number of degrees of freedom is treated dynamically while the remaining degrees of freedom are taken into account by adding the sum of their zero-point energies to the potential along the reaction path. Another more elaborate approach is to constrain the energy in each vibrational mode to be greater than its zero-point value[69,70].

In our purely classical approach we ignore zero-point energies all along the reaction path. But this approach is actually in the spirit of the vibrationally adiabatic approximation. It effectively takes the zero-point energies into account through a shift of the potential along the reaction path corresponding to the sum of all zero-point energies. This shift, however, is constant along the reaction path. Moreover, we still keep the full dimensionality of the problem by explicitly treating all degrees of freedom dynamically. This is indeed essential since for example the steering effect is absent in a low-dimensional treatment of the H_2/Pd(100) system[37,38,39].

Besides zero-point effects tunneling is also an important quantum phenomenon. However, in a system with activated and non-activated paths towards dissociative adsorption tunneling does not play an important role. This is due to the fact that tunneling is exponentially suppressed. Hence the propagation of the quantum particel along a classically possible path is much more probable than the dissociation via tunneling.

The results also show that in purely classical dynamics there is no isotope effect between H_2 and D_2 in the sticking probability. As far as the low-energy regime is concerned, this seems surprising at a first glance, since D_2 is more inert than H_2 due to its higher mass. However, one has to keep in mind that at the same kinetic energy D_2 is slower than H_2, so that there is more time for the steering forces to redirect the D_2 molecule. This has been noted before by Kay *et al.*[42].

Indeed, the Lagrangian for a system of classical particles with the same mass M_1 can be written as

$$L \;=\; \sum_i \; \frac{M_1}{2} \left(\frac{dx_i}{dt} \right)^2 \;-\; U(\{x_i\}) \; . \qquad (16)$$

For another isotope with the mass M_2 the potential does not change. If we transform the time axis via

$$t' \;=\; \sqrt{\frac{M_1}{M_2}} \; t \; , \qquad (17)$$

we end up with the following Lagrangian for the new isotope of mass M_2:

$$L' \;=\; \sum_i \; \frac{M_1}{2} \left(\frac{dx_i}{dt'} \right)^2 \;-\; U(\{x_i\}) \; , \qquad (18)$$

which is equivalent to the Lagrangian of Eq. 16. This means that the equations of motion for an system of classical particles with mass M_1 correspond to the equations of motion for a system of classical particles with mass M_2, where the velocities have been scaled by an factor $\sqrt{\frac{M_1}{M_2}}$, i.e., where the kinetic energy is the same. Hence, for different isotopes with the same initial conditions, where only the initial velocities have been scaled to keep the kinetic energy unchanged, the trajectories remain *exactly* the same.

It follows that there cannot be any isotope effects as a function of the kinetic energy for hydrogen moving classically on a PES as long as there are no energy transfer processes to, e.g., substrate phonons. *Furthermore, this indicates that the steering effect is not restricted to light molecules as hydrogen, but should also be operative for all other heavier molecules moving in a similiar PES.* As far as dissociative adsorption is concerned, however, for heavier molecules recoil effects of the substrate might no longer be negligible, so that for a complete description considering all relevant degrees of freedom energy transfer processes to substrate phonons could be important.

Contrary to the purely classical calculations, the quasiclassical results show an isotope effect between H_2 and D_2. The sticking probability of H_2 is larger compared to D_2, the effect being most pronounced for kinetic energies between 0.03 eV and 0.30 eV. This isotope effect can

only be caused by the different initial vibrational zero-point energies which can be effectively used to traverse the corrugated and anisotropic barrier region. The H_2 gas-phase zero-point energy is larger by 73 meV; indeed the H_2 sticking curve seems to be shifted to lower energies with regard to the D_2 sticking curve by approximately this amount.

Interestingly enough, at very low kinetic energies below 0.03 eV also the quasiclassical calculations show almost no isotope effect, in addition to the fact that classical and quasiclassical results are almost identical in this low-energy range. In the limit of zero initial kinetic energy apparently the sticking probability is to a large extent determined by steering forces which already act rather far away from the surface where the change of the vibrational frequency and thus zero-point effects are insignificant. The absence of an isotope effect for very low energies is actually also true for the averaged quantum results, as Figs. 2 and 3 demonstrate. However, there is a pronounced isotope effect in the quantum results for kinetic energies larger than 0.1 eV. The size of this isotope effect corresponds to the one found in the quasiclassical calculations which again shows that the different initial vibrational zero-point energies cause the isotope effect.

We also like to comment on the rather large difference between classical and quantum results in Fig. 5 for kinetic energies between 0.15 eV and 0.6 eV. We think that this difference might be due to the fact that the sum of all zero-point energies along the minimum energy path through the barrier region actually becomes larger than the gas-phase zero-point energy.[3] This effect is most prominent in the medium energy range, where steering is no longer effective. At very high kinetic energies, where zero-point effects should play only a negligible role, indeed quantum and classical results are in very close agreement. Furthermore, in quantum mechanics it always takes a finite amount of energy to change the state of a particle (if there are no degenerate states), while in classical mechanics particles can be diverted by any infinitesimally small amount of energy. This should make the quantum propagation somehow stiffer than classical propagation. This could also contribute to the difference between quantum and classical results in the medium energy range.

D. Non-normal incidence

In this section we address the issue of non-normal incidence. The experiments on the angular dependence of the sticking probability of H_2/Pd(100) were done for two different initial kinetic energies, $E_i = 0.1$ eV and $E_i = 0.4$ eV.[25] The incident azimuth was not identified. We have determined the quantum and classical angular dependence of the sticking probability for two different incident azimuths: along the [10] direction which corresponds to one axis of the surface square lattice, and along the [11] direction which corresponds to the diagonal of the surface square lattice.

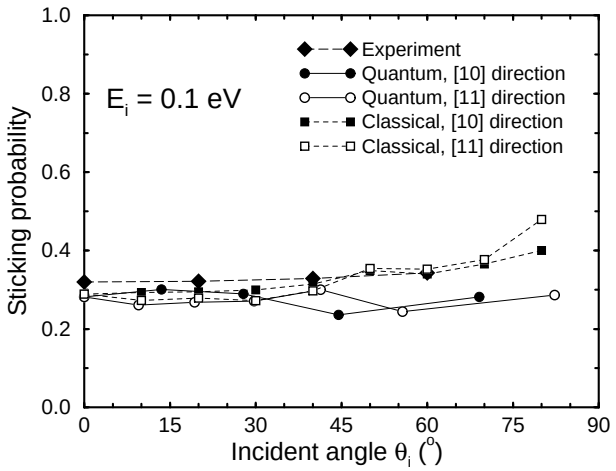

FIG. 6. Probability for dissociative adsorption of H_2 on Pd(100) versus angle of incidence for an inital total kinetic energy of $E_i = 0.1$ eV. Experiment: diamonds (from ref. 25). The theoretical results are for initially non-rotating molecules. Circles show 6D quantum results, squares classical trajectory calculations. The filled and open symbols correspond to calculations with the azimuthal angle of incidence along the [10] and [11] direction of the (100) surface, respectively.

Fig. 6 compares the experiment with the quantum and classical results at the lower kinetic energy, $E_i = 0.1$ eV. Note that the quantum results were determined for a monoenergetic beam in one specific quantum state which is here the vibrational and rotational ground state; hence quantum oscillations are superimposed on these data[8], but apparently their size is small. The general experimental trend is well reproduced by the theoretical results: the sticking probability is almost independent of the angle of incidence at this energy, but slightly increases with increasing angle. There is no large difference between quantum and classical results. Only at angles larger than 45° the classical results are above the quantum results. There is also almost no significant dependence on the azimuth except for the classical results at almost grazing incidence of $\theta_i = 80°$ where the sticking probability along the [11] direction is larger by 0.1 compared to the [10] results.

The angular dependence of the sticking probability at the higher kinetic energy of $E_i = 0.4$ eV is plotted in Fig. 7. First of all the absolut values determined by experiment, quantum and classical calculations are very different at this energy, as is already apparent from Fig. 2 and Fig. 5; this issue was discussed above. But the general trends in the angular dependence are in good agreement. All sets of data show a significant decrease in the sticking probability with increasing incident angle for angles below 60°. For almost grazing incidence there is now a substantial dependence on the initial az-

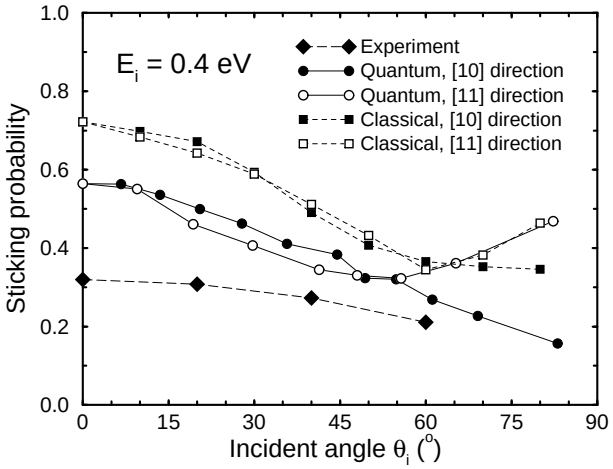

FIG. 7. Probability for dissociative adsorption of H_2 on Pd(100) versus angle of incidence for an inital total kinetic energy of $E_i = 0.4$ eV. The meaning of the symbols is the same as in Fig. 6.

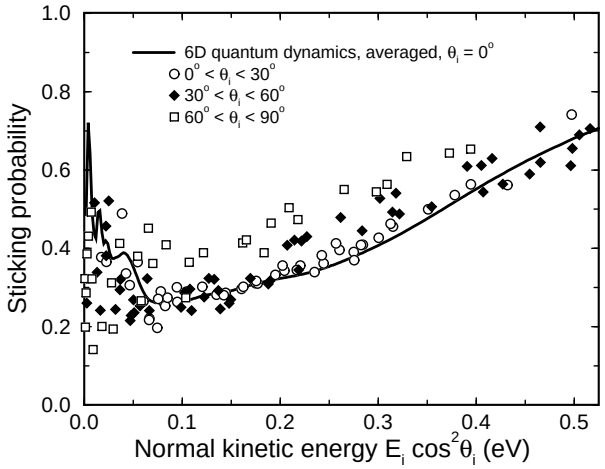

FIG. 8. Quantum mechanical sticking probability of H_2 on Pd(100) as a function of the normal component of the incident energy for molecules initially in the vibrational and rotational ground state. Solid line: beam under normal incidence with an energy spread typical for molecular beam experiments; circles, diamonds, and squares: monoenergetic beam with an angle of incidence between 0° and 30°, between 30° and 60°, and between 60° and 90°, respectively. The results for non-normal incidence are obtained for different azimuthal angles.

imuth. The sticking probability for molecules impinging along the [11] direction is signifincantly larger than for molecules impinging along the [10] direction. This difference is more pronounced for the quantum than for the classical calculations.

Our results show that the general features of the angular dependence of the sticking probability determined in the experiment – an increase with increasing incident angle at low energies and a decrease at higher kinetic energies – is well reproduced by our six-dimensional calculations. In particular, the calculations demonstrate that a sticking probability increasing with increasing incident angle in not necessarily indicative of a precursor mechanism[25] but can be caused by the dynamics of the dissociative adsorption on a corrugated PES.

Still the questions remains: what causes the different angular dependence at these two energies? It is useful to discuss angular effects by considering the energy scaling of the sticking probability[7], i.e., by determining the exponent n such that

$$S(E_i, \theta_i) \approx S(E_i \cos^n \theta_i, \theta_i = 0°) \qquad (19)$$

If $n = 2$, then the so-called normal energy scaling is valid, i.e., the sticking probability is a function of the normal component of the incident energy alone. In our calculations the sticking probability for normal incidence has its minimum at approximately $E_i \approx 0.1$ eV (see Fig. 2). If normal energy scaling were fulfilled in the system H_2/Pd(100), then for $E_i \leq 0.1$ eV the sticking probability would indeed rise with increasing incident angle since the normal energy decreases, and it would fall with increasing angle for $E_i > 0.1$ eV as long as the normal component $E_i \cos^2 \theta_i$ is larger than 0.1 eV.

In order to check whether normal energy scaling is valid in the system H_2/Pd(100), we have plotted the quantum mechanical sticking probability as a function of the normal component of the incident energy $E_i \cos^2 \theta_i$ in Fig. 8. The non-normal incidence data show some scatter, in particular at low energies. This can be caused by quantum oscillations; the azimuthal dependence, which is not specified in Fig. 8, also contributes to the scattering of the data. But the general trends are in qualitative agreement with model calculations on a three-dimensional PES with activated as well as non-activated path towards dissociative adsorption[8]. At low normal kinetic energies below 0.05 eV additional parallel momentum suppresses the sticking, for normal kinetic energies between 0.05 and 0.35 eV additional parallel momentum enhances sticking, and above 0.35 eV the results show approximate normal energy scaling. These results also show that it is not possible to assign any global energy scaling, i.e. any global exponent n in Eq. 19, to the angular dependence of the sticking probability.

At very low energies, where the steering mechanism is operative, additional parallel momentum hinders dissociation. This can be easily understood. A molecule with a low normal velocity may still be steered to a favorable site for dissociation. But due to the additional parallel momentum the molecule is swept past this favorable site and scattered back into the gas-phase from a repulsive site before the bond-breaking can occur. This effect is similiar to the rotational hindering in the steering regime[4,45,72,73,74] which is caused by the fact that

rapidly rotating molecules rotate out of favorable orientation for dissociation during the interaction with the surface. However, Fig. 7 shows that for incident angles above 70° the suppression of the steering depends strongly on the incident azimuth.

In the intermediate energy range between 0.05 and 0.35 eV additional parallel momentum enhances sticking, in particular for incident angles above 60°. For molecules impinging on the surface under an angle larger than 60° the component of the kinetic energy parallel to the surface is at least three times larger than the normal component. These molecules experience an lateral average of the PES in this energy range.[8] Steering in the angular degrees of freedom can still occur. Indeed the sticking probability for $\theta_i > 60°$ shows a decrease for normal kinetic energies between 0.05 eV and 0.12 eV indicating a steering effect, and then an increase at higher energies. Far away from the surface the molecules are first attracted to the on-top-site[41]. But molecules steered to this site will eventually encounter a barrier towards dissociative adsorption of 0.15 eV. In order to dissociate slow molecules have to be re-directed towards the bridge or hollow sites (see also Ref. 44). Thus potential gradients can also steer molecules to "wrong" sites. This oversteering in the lateral coordinates cannot occur for molecules experiencing a laterally averaged potential causing the increase in the sticking probability for large additional parallel momentum.

In the direct dissociation regime for normal kinetic energies larger than the lateral average of the barrier height additional parallel momentum causes an increase in the sticking probability.[8] This lateral average still depends on the orientation of the molecule. For the majority of molecular orientations the laterally averaged barrier heights for H_2/Pd(100) are less than 0.15 eV (see, e.g., the barrier distribution in Ref. 46). Hence the lateral averaging also leads to an increase in the sticking probability in the direct dissociation regime.

This mechanism, however, does not promote sticking significantly any more if the normal kinetic energy is larger than most of the maximum barriers for fixed molecular orientation. Still, the fact that for $E_i \cos^2 \theta_i > 0.35$ eV the sticking probability shows approximate normal energy scaling in spite of the strong corrugation of the PES is reminiscent of the activated system H_2/Cu. There similiar results have been found both experimentally[11,13] and theoretically[20] although the PES is also strongly corrugated[75,76]. This apparent contradiction is attributed to features of the PES called balanced corrugation[7,77,78]. For this type of corrugation the higher barriers have to be farther away from the surface compared to the lower barriers. These features are also present in the system H_2/Pd(100) where the highest barriers are over the on-top-sites[41].

We now return to the discussion of the angular dependence of the sticking probability for fixed total kinetic energy. For fixed total kinetic energy increasing the incident angle means decreasing the normal kinetic energy and increasing the incident parallel momentum. At low kinetic energies decreasing the normal kinetic energy makes the steering more effective which promotes dissociation. On the other hand, increasing the incident parallel momentum hinders dissociation in the low-energy range. At $E_i = 0.1$ eV both effects approximately cancel which leads to a sticking probability almost independent of the incident angle (see Fig. 6).

At normal energies larger than 0.1 eV decreasing the normal kinetic energy leads to a decrease in the sticking probability, but increasing the incident angle enhances the sticking probability for normal energies below 0.4 eV. However, the promoting effect of additional parallel momentum is less pronounced than the decrease due to the smaller normal kinetic energy. Hence in Fig. 7 the sticking probability decreases for increasing incident angle at an initial total kinetic energy of 0.4 eV.

Figs. 6 and 7 also show that for $\theta_i < 60°$ there is almost no dependence of the sticking probability for non-normal incidence on the azimuth. For larger incident angles, however, molecules impinging along the [11] direction of the surface unit cell have a higher dissociation probability than molecules impinging along the [10] direction. This can be explained by a shadowing effect. For molecules approaching the surface under an almost grazing incidence along one axis of the quadratic surface unit cell, the most favorable adsorption path at the bridge position is effectively hidden behind the high barriers at the on-top position. For an approach along the diagonal of the square unit cell this most favorable adsorption path is still directly accessible.

Finally we study the influence of the incident rotational quantum state on the angular dependence of the sticking probability. We have determined the sticking probability as a function of the angle of incidence for molecules initially in the rotational quantum state $j_i = 2, m_i = 0$ and $j_i = 2, m_i = 2$ for $E_i = 0.1$ eV. The results are plotted in Fig. 9. Note that for $\theta_i = 0°$ the sticking probability for initially non-rotating molecules with $j_i = 0$ is 0.3 (see Fig. 6). Fig. 9 shows the well-known result[4,45,72,73,74] that rotational motion hinders the dissociation at low energies because rotating molecules rotate out of favorable orientations for dissociation. This suppression, however, depends on the orientation of the molecules. Molecules with azimuthal quantum number $m = j$ have their axis preferentially oriented parallel to the surface. These molecules rotating in the so-called helicopter fashion dissociate more easily than molecules rotating in the cartwheel fashion ($m = 0$) where the rotational axis is preferentially oriented parallel to the surface. The latter have a high probability hitting the surface in an upright orientation in which they cannot dissociate.

This steric effect is effective for all incident angles, i.e., the sticking probability for $m_i = 2$ is always larger than for $m_i = 0$. Like for the non-rotating molecules at this kinetic energy, the results show only a weak dependence on the incident angle. For incident angles below 45° there is also no significant dependence on the azimuth, but again,

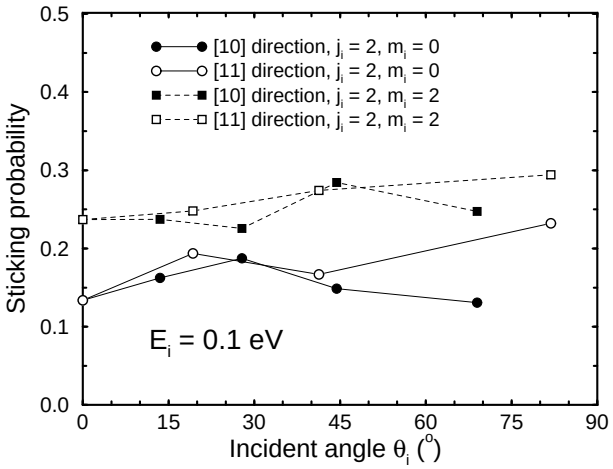

FIG. 9. Quantum dynamical probability for dissociative adsorption of H_2 on Pd(100) versus angle of incidence for an inital total kinetic energy of $E_i = 0.1$ eV. The results are for molecules initially in the rotational quantum state $j = 2$. Circles show results for initial rotational azimuthal quantum number $m_i = 0$, squares for $m_i = 2$. The filled and open symbols correspond to calculations with the azimuthal angle of incidence along the [10] and [11] direction of the (100) surface, respectively.

for almost grazing incidence molecules approaching along the diagonal of the surface unit cell have a higher dissociation probability than molecules approaching along one axis of the surface unit cell. These results indicate that to first order rotational and parallel motion are decoupled as far as the dissociation dynamics is concerned.

IV. CONCLUSIONS

In conclusion, we reported a six-dimensional quantum and classical dynamical study of dissociative adsorption of hydrogen on Pd(100). We used a potential energy surface obtained from detailed density functional theory calculations for the system H_2/Pd(100). The six hydrogen degrees of freedom are treated fully dynamically. The two main approximations are, firstly, that the substrate is kept fixed so that no thermal disorder or phonon excitations are allowed, and secondly, that the system is assumed to remain in its electronic ground state. Hence the continuous excitation spectrum of the semi-infinite substrate is neglected. Still these calculations are able to reproduce all of the known experimental results with regard to the disscociative adsorption at least semi-quantitatively. The time-reverse process to dissociative adsorption, the associative desorption, was not discussed in this study, but previous studies showed that also experimental desorption properties are well-reproduced by our calculations. Among the processes that are now quite well understood are the dependence of adsorption and/or desorption on the molecular translational energy, vibrational and rotational state, orientation of the molecule, and the angle of incidence.

Quantum effects are non-neglible for hydrogen dissociation on surfaces. The discrete nature of diffraction and molecular excitation leads to a strong oscillatory structure of the sticking probability as a function of the incident kinetic energy. Furthermore, zero-point effects cause substantial deviations between *averaged* quantum dynamical calculations and quasiclassical calculations, in which the initial conditions correspond to a molecule vibrating with the gas-phase zero-point energy of hydrogen. The corrugated and anisotropic potential energy surface leads to the building up of additional zero-point energies which effectively increase the minimum potential in the quantum calculations. This changes the dynamics in the low-energy regime of H_2/Pd(100) dramatically. However, the building up of the additional zero-point energies roughly cancels and even overcompensates the decrease in the zero-point energy of the H-H vibrations upon dissociative adsorption. Therefore purely classical calculations which neglect the zero-point energies in the initial conditions are closer to the quantum results than the quasiclassical calculations.

At low kinetic energies the dissociative adsorption is dominated by the steering effect. For higher kinetic energies steering becomes less efficient leading to the initial decrease in the sticking probability. The steering effect is dependent on the kinetic energy, but not on the mass of the molecule. Hence steering should also be effective for heavier molecules.

There are still some quantitative differences between theory and experiment. They might be caused by uncertainties in the evaluation of the PES, but also by uncertainties in the experimental determination of the sticking probability. In addition, the differences might be caused by the neglect of substrate phonons or electronic excitations in the calculations. Hence we will address the role of the substrate degrees of freedom in the adsorption and desorption processes in the future. As for now, our results show that the *ab initio* determination of the potential energy surface combined with high-dimensional dynamical calculations, in which the relevant degrees of freedon are taken into account, is an important step forward in our understanding of simple reactions at surfaces.

[1] A. De Vita, I. Štich, M.J. Gillan, M.C. Payne, and L.J. Clarke, Phys. Rev. Lett. **71**, 1276 (1993).
[2] A. Gross, M. Bockstedte, and M. Scheffler, submitted.
[3] A. Gross and M. Scheffler, to appear in J. Vac. Sci. Technol.
[4] A. Gross, S. Wilke, and M. Scheffler, Phys. Rev. Lett. **75**, 2718 (1995).
[5] K.D. Rendulic and A. Winkler, Surf. Sci. **299/300**, 261

(1994).
[6] S. Holloway, Surf. Sci. **299/300**, 656 (1994).
[7] G.R. Darling and S. Holloway, Rep. Prog. Phys. **58**, 1595 (1995).
[8] A. Gross, J. Chem. Phys. **102**, 5045 (1995).
[9] A. Gross, Surf. Sci. **363**, 1 (1996).
[10] B.E. Hayden and C.L.A. Lamont, Phys. Rev. Lett. **63**, 1823 (1989).
[11] G. Anger, A. Winkler, and K.D. Rendulic, Surf. Sci. **220**, 1 (1989).
[12] A. Hodgson, J. Moryl, P. Traversaro, and H. Zhao, Nature **356**, 501 (1992).
[13] C.T. Rettner, D.J. Auerbach, and H.A. Michelsen, Phys. Rev. Lett. **68**, 1164 (1992).
[14] C.T. Rettner, H.A. Michelsen, and D.J. Auerbach, J. Chem. Phys. **102** (1995), 4625.
[15] S. Küchenhoff, W. Brenig, and Y. Chiba, Surf. Sci. **245**, 389 (1991).
[16] G.R. Darling and S. Holloway, J. Chem. Phys. **97**, 734 (1992).
[17] R.C. Mowrey, J. Chem. Phys. **99**, 7049 (1993).
[18] G. R. Darling and S. Holloway, J. Chem. Phys. **101**, 3268 (1994).
[19] T. Brunner and W. Brenig, Surf. Sci. **317**, 303 (1994).
[20] A. Gross, B. Hammer, M. Scheffler, and W. Brenig, Phys. Rev. Lett. **73**, 3121 (1994).
[21] S. Kumar and B. Jackson, J. Chem. Phys. **100**, 5956 (1994).
[22] J. Dai and J. Z. H. Zhang, J. Chem. Phys. **102**, 6280 (1995).
[23] G.J. Kroes, G. Wiesenekker, E.J. Baerends, and R.C. Mowrey, Phys. Rev. B **53**, 10397 (1996).
[24] W.A. Diño, H. Kasai, and A. Okiji, Phys. Rev. Lett. **78**, 286 (1997).
[25] K. D. Rendulic, G. Anger, and A. Winkler, Surf. Sci. **208**, 404 (1989).
[26] Ch. Resch, H. F. Berger, K. D. Rendulic, and E. Bertel, Surf. Sci. **316**, L1105 (1994).
[27] H. F. Berger, Ch. Resch, E. Grösslinger, G. Eilmsteiner, A. Winkler, and K. D. Rendulic, Surf. Sci. **275**, L627 (1992)
[28] D. A. Butler, B. E. Hayden, and J. D. Jones, Chem. Phys. Lett. **217**, 423 (1994).
[29] P. Alnot, A. Cassuto, and D. A. King, Surf. Sci. **215**, 29 (1989).
[30] D. A. Butler and B. E. Hayden, Surf. Sci. **337**, 67 (1995).
[31] St. J. Dixon-Warren, A. T. Pasteur, and D. A. King, Surf. Rev. and Lett. **1**, 593 (1994).
[32] A.C. Luntz, M.D. Williams, and D.S. Bethune, J. Chem. Phys. **89**, 4381 (1988).
[33] J.M. Bradley, X.-C. Guo, A. Hopkinson, and D.A. King, J. Chem. Phys. **104**, 4283 (1996).
[34] C.T. Rettner, L.A. DeLouise, and D.J. Auerbach, J. Chem. Phys. **85**, 1131 (1986).
[35] M.C. Wheeler, D.C. Seets, and C.B. Mullins, J. Chem. Phys. **105**, 1572 (1996).
[36] C.T. Rettner, H. Stein, and E.K. Schweizer, J. Chem. Phys. **89**, 3337 (1988).
[37] L. Schröter, S. Küchenhoff, R. David, W. Brenig, and H. Zacharias, Surf. Sci. **261** (1992) 243.
[38] G. R. Darling and S. Holloway, Surf. Sci. **268**, L305 (1992).
[39] W. Brenig and R. Russ, Surf. Sci. **315**, 195 (1994).
[40] D.A. King, CRC Rev. Solid State Mater. Sci. **7**, 167 (1978).
[41] S. Wilke and M. Scheffler, Surf. Sci. **329**, L605 (1995); Phys. Rev. B **53**, 4926 (1996).
[42] M. Kay, G.R. Darling, S. Holloway, J.A. White, and D.M. Bird, Chem. Phys. Lett. **245**, 311 (1995).
[43] J.A. White, D.M. Bird, and M.C. Payne, Phys. Rev. B **53**, 1667 (1996).
[44] A. Eichler, G. Kresse, and J. Hafner, Phys. Rev. Lett. **77**, 1119 (1996).
[45] A. Gross, S. Wilke, and M. Scheffler, Surf. Sci. **357/358**, 614 (1996).
[46] A. Gross and M. Scheffler, Chem. Phys. Lett. **256**, 417 (1996).
[47] A. Gross and M. Scheffler, Prog. Surf. Sci. **53**, 187 (1996).
[48] A. Gross and M. Scheffler, Chem. Phys. Lett. **263**, 567 (1996).
[49] G.L. Hofacker, Z. Naturforsch. **18a**, 607 (1963).
[50] R.A. Marcus, J. Chem. Phys. **41**, 2614 (1964).
[51] W. Brenig and H. Kasai, Surf. Sci. **213**, 170 (1989).
[52] G. Wiesenekker, G.J. Kroes, and E.J. Baerends, J. Chem. Phys. **104**, 7344 (1996).
[53] J. P. Perdew J. A. Chevary, S. H. Vosko, K. A. Jackson, M. R. Pederson, D. J. Singh, and C. Fiolhias, Phys. Rev. B **46**, 6671 (1992).
[54] B. Kohler, S. Wilke, M. Scheffler, R. Kouba, and C. Ambrosch-Draxl, Comp. Phys. Comm. **94**, 31 (1996).
[55] H. Haken and H.C. Wolf, *Molecular Physics and Elements of Quantum Chemistry* (Springer, Berlin, 1995), p.175.
[56] W. Brenig, T. Brunner, A. Gross, and R. Russ, Z. Phys. B **93**, 91 (1993).
[57] G.J. Kroes, J.G. Snijders, and R.C. Mowrey, J. Chem. Phys. **103**, 5121 (1995).
[58] Y. Chiba, Ph.D. thesis, University of Tokyo, 1993.
[59] W.H. Press, B.P. Flannery, S.A. Teukolsky, and W.T. Vetterling, *Numerical Recipes*, Cambridge University Press, Cambridge, 1989.
[60] R. Frisch and O. Stern, Z. Phys. **84**, 430 (1933).
[61] J.B. Pendry, *Low energy electron diffraction*, Academic Press, London (1974), p. 112.
[62] C.T. Rettner and D.J. Auerbach, Phys. Rev. Lett. **77**, 404 (1996).
[63] A. Gross and M. Scheffler, Phys. Rev. Lett. **77**, 405 (1996).
[64] C.T. Rettner and D.J. Auerbach, Chem. Phys. Lett. **253**, 236 (1996).
[65] M. R. Hand and J. Harris, J. Chem. Phys. **92**, 7610 (1990).
[66] A. Gross, Surf. Sci. **320**, L68 (1994).
[67] B. Hammer, K.W. Jacobsen and J.K. Nørskov, Phys. Rev. Lett. **69**, 1971 (1992).
[68] P. Kratzer, B. Hammer, and J.K. Nørskov, Chem. Phys. Lett. **229**, 645 (1994); Phys. Rev. **B 51**, 13432 (1995).
[69] J.M. Bowman. B. Gazdy, and Q. Sun, J. Chem. Phys. **91**, 2859 (1989).
[70] W. H. Miller, W. L. Hase, and C. L. Darling, J. Chem. Phys. **91**, 2863 (1989).
[71] *The Theory of Chemical Reactions Dynamics*, ed. by D. C. Clary, Reidel, Dordrecht, 1986.
[72] M. Beutl, M. Riedler, and K.D. Rendulic, Chem. Phys. Lett. **247**, 249 (1995).
[73] M. Beutl, M. Riedler, and K.D. Rendulic, Chem. Phys. Lett. **256**, 33 (1996).

[74] M. Gostein and G.O. Sitz, subm. to J. Chem. Phys.
[75] B. Hammer, M. Scheffler, K.W. Jacobsen, and J.K. Nørskov, Phys. Rev. Lett. **73**, 1400 (1994).
[76] J.A. White, D.M. Bird, M.C. Payne, and I. Stich, Phys. Rev. Lett. **73**, 1404 (1994).
[77] G.R. Darling and S. Holloway, Surf. Sci. **304**, L461 (1994).
[78] W. Brenig, A. Gross, and R. Russ, Z. Phys. **B** 97, 311 (1995).